CrossMark

HIP

Correlation of alpha angle between various radiographic projections and radial magnetic resonance imaging for cam deformity in femoral head–neck junction

Masayoshi Saito[1] · Sachiyuki Tsukada[1] · Kazuki Yoshida[2] · Yasuaki Okada[1] · Atsushi Tasaki[1]

Abstract

Purpose Radial magnetic resonance imaging (MRI) along the axis of the femoral head neck is the gold standard for detection of cam deformity of the proximal femur. This study was performed to identify which plain radiographic projection was best correlated with radial MRI.

Methods Five different plain radiographic projections and 18 slices of radial MRI were applied to 35 consecutive hips with groin pain and positive impingement sign. Alpha angles were measured to detect the asphericity of the femoral head–neck junction in all images. Radiographs were taken in anteroposterior pelvis, cross-table lateral, 90° Dunn, 45° Dunn and modified 45° Dunn views. Pearson's correlation coefficients were determined to assess the association between the alpha angle obtained from radial MRI and each radiographic technique. The sensitivity, specificity, positive and positive predictive values and accuracy of plain radiographic alpha angle measurements were assessed using a threshold alpha angle value of 50.5° for cam deformity.

Results Pearson's correlation coefficients in the alpha angle values between MRI and plain radiographic projections were 0.45, 0.70, 0.62, 0.81 and 0.69 for the anteroposterior pelvis, cross-table lateral, 90° Dunn, 45° Dunn and modified 45° Dunn views, respectively. In terms of sensitivity and accuracy, the 45° Dunn view had the greatest values.

Conclusions Alpha angle of the 45° Dunn view was best correlated with that of radial MRI. The 45° Dunn view had better sensitivity and accuracy than other radiographic projections. The 45° Dunn view may be preferable for screening of cam deformity.

Level of evidence II.

Keywords Hip · Cam · Femoroacetabular impingement · Radiology

Introduction

Cam-type femoroacetabular impingement (FAI) is characterised as a consequence of a malshaped proximal femur and is associated with hip osteoarthritis [10, 11, 20]. Although magnetic resonance imaging (MRI) radial slices are considered the gold standard for detection of cam deformity [12, 15, 16, 19], plain radiographic images are used most frequently in clinical settings [8, 17].

In 1952, Dunn compared the utility of 33 plain radiographic projections including various hip positions using a 3-year-old femur model to assess femoral neck anteversion [9]. Barton et al. [1] compared the correlation of alpha angle of MRI and those of three plain radiographic projections, i.e. anteroposterior (AP) pelvis view, cross-table lateral view and 90° Dunn view (with hip flexed at 90° and abducted 20°), and concluded that the alpha angle of the 90° Dunn view showed the best correlation with that of MRI. Meyer et al. [17] reported that another Dunn view—45° Dunn view, with hip flexed at 45° and abducted 20°—was more sensitive than the 90° Dunn view for detection of asphericity of the proximal femur. Therefore, it remains

✉ Sachiyuki Tsukada
  s8058@nms.ac.jp

1 Department of Orthopaedic Surgery, St. Luke's International Hospital, 9-1 Akashicho, Chuo-ku, Tokyo 104-8560, Japan

2 Department of Epidemiology, Harvard T. H. Chan School of Public Health, 677 Huntington Ave, Boston, MA 02115, USA

🙲 Springer

unclear which projections have the best correlations with MRI.

The alpha angles of five plain radiographic projections were compared to determine which showed the best correlation to the alpha angle of radial MRI. The hypothesis of this study was that the 45° Dunn view would be best correlated with radial MRI compared to other plain radiographic projections.

Materials and methods

Setting and participants

This study was performed at the orthopaedics department of a single general hospital. Patients with groin pain with impingement sign and a diagnosis of hip labral tear based on MRI radial slices between January 2014 and September 2014 were included in the study. During the study period, patients were routinely investigated for femoroacetabular impingement via five plain radiographic projections, i.e. AP pelvis, cross-table lateral, 90° Dunn, 45° Dunn and modified 45° Dunn views. Patients with osteoarthritis of more than Tönnis grade 1 or acetabular dysplasia with lateral centre edge angle less than 25° were excluded [5]. Other exclusion criteria were osteonecrosis, prior hip surgery, post-traumatic hip disorder, residual paediatric hip disease (slipped capital femoral epiphysis or Legg–Calvé–Perthes disease) or inadequate plain radiographic images (i.e. not well centred or the patient's pelvis was rotated).

Roentgenography and measurement

Plain radiographic images were taken by radiology technologists using standardised techniques. Radiographs were taken in five different projections: plain AP pelvis view, cross-table lateral view, 90° Dunn view, 45° Dunn view and modified 45° Dunn view. The AP pelvis view was taken with the patient in the supine position on the radiographic table with both lower extremities oriented at internal rotation of 15° [6]. The cross-table lateral view was taken with the patient in the supine position on the radiographic table with the contralateral hip and knee flexed beyond 80° and the symptomatic limb internally rotated by 15° to expose the anterolateral surface of the femoral head–neck junction [6]. The 90° Dunn view was taken with the patient in the supine position with the symptomatic hip flexed at 90° and abducted 20° in neutral rotation [5, 9, 17]. The 45° Dunn view was taken with the patient in the supine position with the symptomatic hip flexed at 45° and abducted 20° in neutral rotation [5, 9, 17]. The modified 45° Dunn view was taken with the patient in the supine position with the symptomatic hip flexed at 45° and abducted 45° in neutral rotation [9].

Two assessors (MS and YO) measured the alpha angles of five plain radiographic projections in a blinded manner using computer software (Two-Dimensional Template; Japan Medical Material, Osaka, Japan) (Fig. 1). Although the computer software could measure the angle to two decimal places, we truncated the number to one decimal place to minimise measurement error. To measure the alpha angle, two arms of the angle were determined [18]; the first arm of the angle was the long axis of the femoral neck, while the second arm was drawn from the centre of the best fit circle anteriorly to the point where the head extended beyond the margin of the circle. The alpha angle thus formed provided a quantitative measurement of the degree of femoral head asphericity and/or lack of head–neck junction offset and/or concavity. In radiographic assessment, the cam lesion was defined as alpha angle >50.5° on the image, as reported previously [1].

MRI examination was performed with the patient in the supine position with lower extremities oriented at internal rotation of 15°. All images were acquired using a 3.0-tesla scanner (Discovery MR750w 3T; GE Healthcare, Wauwatosa, WI, USA) with a flexible surface coil. Among the series of coronal reconstructed images, the edges of the acetabular labrum were identified in the slice that demonstrated the midpoint of the femoral head (Fig. 2a). The slice connecting the edges of the acetabular labrum on this coronal image was reconstructed and set as the reference plane to reconstruct the radial MRI (Fig. 2b). Then, radial slices passing through the midpoint of the femoral head were reconstructed along the axis of the femoral neck. The locations of the slices in the sequence were described in a clockwise manner, with 3, 6, 9 and 12 o'clock corresponding to anterior, inferior, posterior and superior, respectively [12]. The most prominent contour of the femoral greater trochanter was defined as the 12 o'clock position of the femoral head–neck junction [12]. The radial slices were translated into hourly orientation starting from the 12 o'clock position. Each slice corresponded to 10 angular minutes (Fig. 2c).

The two assessors also measured the alpha angle obtained by radial MRI. They measured the alpha angle on 18 slices of radial MRI around the femoral head–neck junction (Fig. 2c). At each slice, the alpha angle was measured using the same technique as described above (Fig. 3). The greatest value in the series of 18 radial slices of MRI was determined as the alpha angle of the radial MRI in the hip (Fig. 3). In addition to the value of the alpha angle, the location at which the alpha angle showed the greatest value was assessed. In the MRI assessment, the cam lesion was also defined as alpha angle >50.5° on the image as reported previously [1].
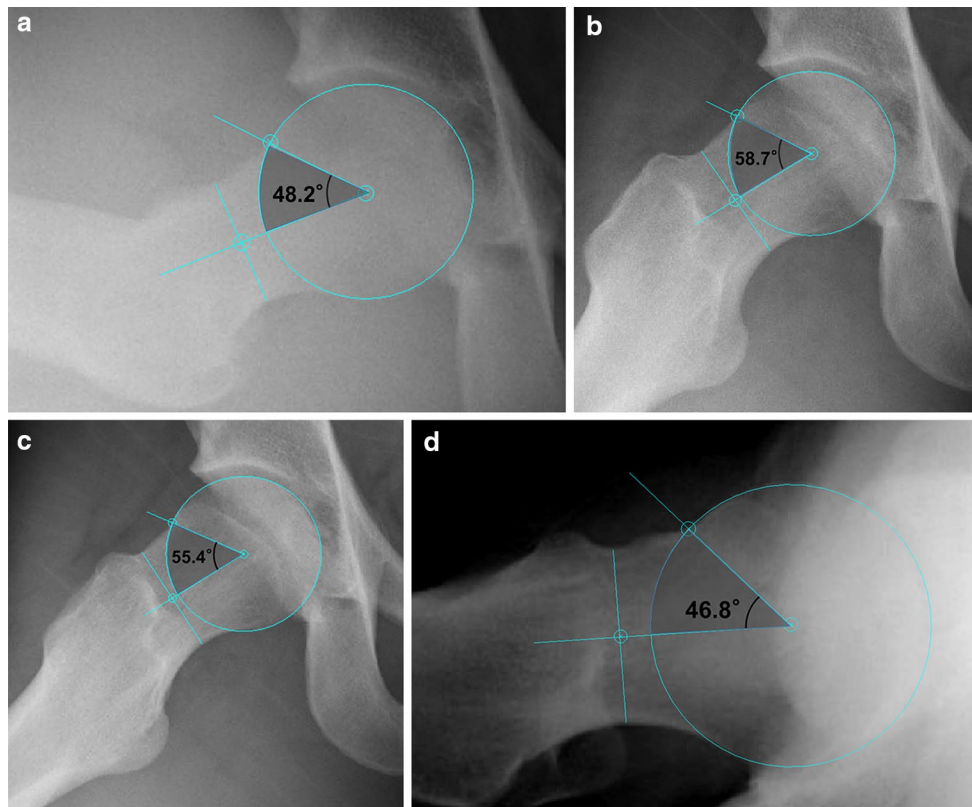
Fig. 1 Measurement of alpha angle on plain radiographs obtained in different radiographic projections. **a** The 90° Dunn view, taken with the patient in the supine position with the symptomatic hip flexed at 90° and abducted 20°, with an alpha angle of 48.2°. **b** The 45° Dunn view, taken with the patient in the supine position with the symptomatic hip flexed at 45° and abducted 20°, with an alpha angle of 58.7°. **c** The modified 45° Dunn view, taken with the patient in the supine position with the symptomatic hip flexed at 45° and abducted 45°, with an alpha angle of 55.4°. **d** The cross-table lateral view, taken with the patient in the supine position with the contralateral hip and knee flexed beyond 80° and the symptomatic limb internally rotated 15°, with an alpha angle of 46.8°

Compliance with ethical standards

The study protocol and publication were approved by the ethics committee of St. Luke's International Hospital (registration number 15-R032).

Statistical analyses

The Pearson's correlation coefficients were determined to assess the association between the alpha angle obtained from radial MRI and each radiographic technique. The sensitivity, specificity, positive predictive value, negative predictive value and accuracy of the plain radiographic alpha angle measurements were calculated using a threshold alpha angle value of 50.5° as measured on radial MRI. To test interobserver reliability, the intraclass correlation coefficients (ICC) of radial MRI and five projections were calculated for two assessors.

The sample size of this study was all of the available data. To accurately describe the uncertainty in our results,

95 % confidence intervals to the correlation coefficients and test performance measures were added.

All statistical analyses were performed by an investigator (ST) using R (The R Foundation for Statistical Computing).

Results

Of the total of 55 consecutive patients with 59 involved hips screened for eligibility, 34 patients with 35 involved hips were included in the study. The flow chart presented in Fig. 4 outlines the study. Four patients with osteoarthritis of more than Tönnis grade 1 and nine patients with acetabular dysplasia with lateral canter edge angle <25° were excluded. In addition, one patient with residual paediatric hip disease (Legg–Calvé–Perthes disease) and 10 patients with inadequate plain radiographic images were excluded. The patients included in this study had a median age of 52 years (range 17–76 years) and consisted of 19 males
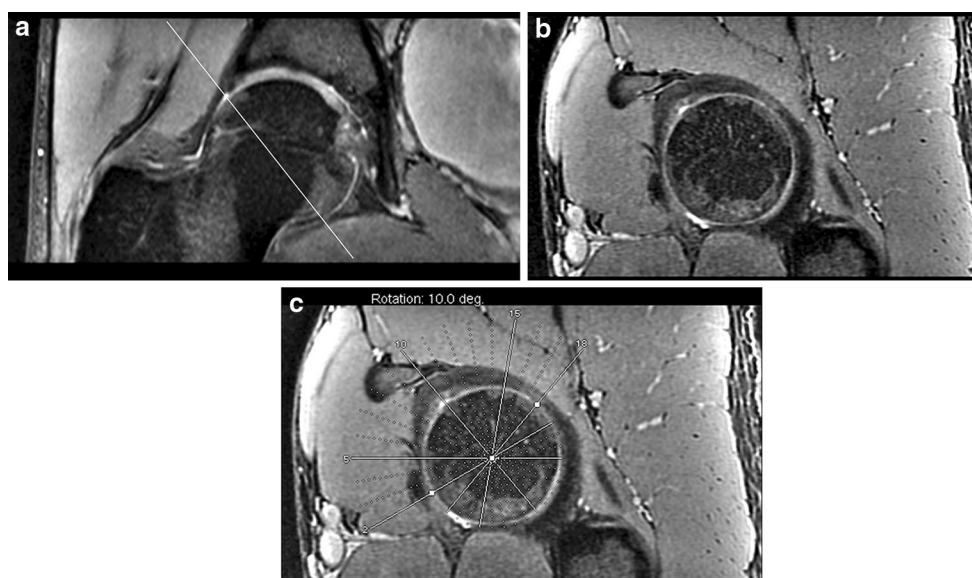
Fig. 2 Reconstruction of radial magnetic resonance images for evaluation. **a** The magnetic resonance image that best demonstrated the midpoint of the femoral head in the sequence of coronal images. The edges of the acetabular labrum were identified on this image (*white line*). **b** Slice corresponding to the white line in **a**. **c** Radial slice localisation depicted in **b**. The *white dotted line* indicates slices cut at 10 angular minutes. Two *white lines* with *white squares* indicate the starting line (line 2) and ending line (line 18), respectively. *White lines* without *white squares* indicate each fifth line (i.e. lines 5, 10 and 15)
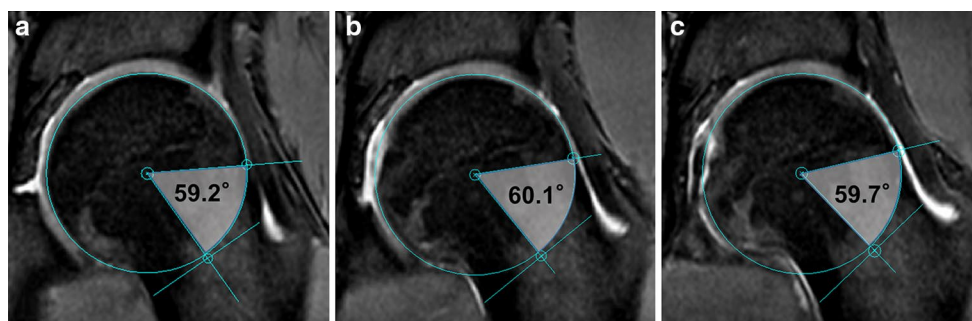

Fig. 3 Measurement of alpha angle on each radial MRI slice. Alpha angle of this hip was 60.1°, the greatest value in the series measurement of all slices. **a** A radial slice at the 2:40 clock position at the femoral neck axis with alpha angle of 59.2° (line 5 in Fig. 2). **b** A radial slice at 2:20 clock position at the femoral neck axis with alpha angle of 60.1° (line 6 in Fig. 2). **c** A radial slice at 2:00 clock position at the femoral neck axis with alpha angle of 59.7° (line 7 in Fig. 2)

and 15 females with involvement of 17 left and 18 right hips.

Table 1 shows the alpha angles obtained from each image and the Pearson's correlation coefficients for the alpha angle values between MRI as the gold standard and the plain radiographic projections. In the radial MRI slices, the greatest value of alpha angle was located anterosuperiorly (between 12 o'clock and 3 o'clock in clockwise rotation; range 12:20–2:40) in all patients.

Cam deformity with alpha angle >50.5° was detected in 33 of 35 hips on radial MRI. The cam deformity was present in two hips on the AP pelvis view, in 15 hips on the cross-table lateral view, in 18 hips on the 90° Dunn view, in 29 hips on the 45° Dunn view and in 25 hips on the modified 45° Dunn view. The sensitivity, specificity, specificity, positive predictive value, negative predictive value and accuracy are shown in Table 2.

The interobserver reliabilities for all measurements are shown in Table 3.

Discussion

The most important finding of this study was that the 45° Dunn view was most closely correlated with radial MRI compared with the AP pelvis, cross-table lateral, 90° Dunn
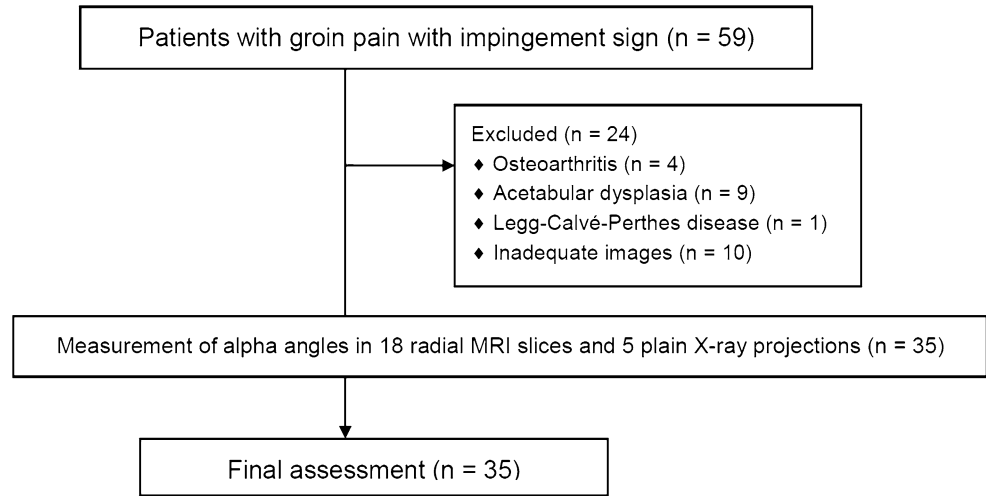
Fig. 4 Patient flow diagram

Patients with groin pain with impingement sign (n = 59)

Excluded (n = 24)
- Osteoarthritis (n = 4)
- Acetabular dysplasia (n = 9)
- Legg-Calvé-Perthes disease (n = 1)
- Inadequate images (n = 10)

Measurement of alpha angles in 18 radial MRI slices and 5 plain X-ray projections (n = 35)

Final assessment (n = 35)

Table 1 Alpha angle obtained from each view and Pearson's correlation coefficients compared to radial MRI

	Radial MRI	AP pelvis view	Cross-table lateral view	90° Dunn view	45° Dunn view	Modified 45° Dunn view
Alpha angle, degree	59 ± 7; range 48–74	45 ± 6; range 36–71	50 ± 6; range 40–66	51 ± 6; range 40–62	58 ± 7; range 45–72	55 ± 7; range 45–68
Pearson's correlation coefficient[a]	1	0.45 (0.14–0.68)	0.70 (0.48–0.84)	0.62 (0.36–0.79)	0.81 (0.66–0.90)	0.69 (0.46–0.83)

AP anteroposterior, *MRI* magnetic resonance imaging

[a] 95 % Confidence intervals are given in parentheses

Table 2 Comparison of sensitivity, specificity, positive predictive value, negative predictive value and accuracy of the five views in comparison with radial MRI

	AP pelvis view	Cross-table lateral view	90° Dunn view	45° Dunn view	Modified 45° Dunn view
Sensitivity[a]	0.06 (0.07–0.20)	0.46 (0.28–0.64)	0.52 (0.34–0.69)	0.82 (0.65–0.93)	0.73 (0.55–0.87)
Specificity[a]	1 (0.09–1)	1 (0.09–1)	0.50 (0.01–0.99)	0 (0–0.91)	0.5 (0.01–0.99)
Positive predictive value[a]	1 (0.09–1)	1 (0.70–1)	0.94 (0.73–1)	0.93 (0.77–0.99)	0.96 (0.8–1)
Negative predictive value[a]	0.06 (0.01–0.20)	0.10 (0.01–0.32)	0.06 (0.01–0.99)	0 (0–0.58)	0.1 (0–0.45)
Accuracy[a]	0.11 (0.03–0.20)	0.49 (0.31–0.66)	0.51 (0.34–0.69)	0.77 (0.60–0.90)	0.71 (0.54–0.85)

AP anteroposterior, *MRI* magnetic resonance imaging

[a] 95 % Confidence intervals are given in parentheses

Table 3 Intraclass correlation coefficients of radial MRI and five projections by two independent observers

	Radial MRI	AP pelvis view	Cross-table lateral view	90° Dunn view	45° Dunn view	Modified 45° Dunn view
Intraclass correlation coefficients[a]	0.92 (0.84–0.96)	0.79 (0.39–0.92)	0.88 (0.78–0.94)	0.83 (0.69–0.91)	0.93 (0.87–0.96)	0.88 (0.78–0.94)

AP anteroposterior, *MRI* magnetic resonance imaging

[a] 95 % Confidence intervals are given in parentheses

and modified 45° Dunn views. In addition, the 45° Dunn view had the greatest values of sensitivity for cam lesion detection on MRI.

Many investigators recommend radial MRI slices along the axis of the femoral head neck to examine the circumference of the femoral head–neck junction [8, 12, 15, 16, 19]. Barton et al. [1] concluded that the alpha angle of the 90° Dunn view was most closely correlated to that of MRI. However, MRI measurement was used with oblique axial images [1]. In our study, using radial MRI slices along the axis of the femoral neck, the Pearson's correlation coefficient in the alpha angle values between the MRI and the 45° Dunn view was 0.81 (highly correlated) and better than other projections, including the 90° Dunn view.

The reason why the 45° Dunn view had the best correlation to the radial MRI might have been because the cam lesion was located in the anterosuperior area of the head–neck junction (between 12:20 and 2:40) in all patients included in this study. Previous studies revealed that cam lesions are most common in the anterosuperior area [7, 8], and 45° Dunn view was superior to detect the cam lesion in this area [7]. However, despite the low frequency, cam lesions located in areas other than the anterosuperior area are also clinically important, such as the posterior-based cam, which is considered to be a relative contraindication of arthroscopic surgery [14].

There were questions regarding whether the 45° Dunn view had better sensitivity than the 90° Dunn view [1, 17]. Our results indicated that the 45° Dunn view had better sensitivity than other radiographic projections. Therefore, the 45° Dunn view may be more suitable for screening of cam deformity on radiographs than the 90° Dunn view, which is the current standard Dunn view [17].

Physicians should take care as the 45° Dunn view did not show the greatest specificity compared with other plain radiographic projections, and the most suitable projection should be chosen in each clinical setting.

Our study had several limitations. First, although we attempted to ensure that all radiographs and MRIs were taken with standardised hip joint position, some variation of hip position may have occurred, which could have distorted the results. Second, despite the standardisation of technique to reconstruct radial MRI slices, determination of the locations of the slices could be limited in terms of accuracy. Acknowledging this limitation, we believe that our study still has important clinical relevance because the measurement error was not large to change the fact that all study patients had the greatest value of alpha angle in the anterosuperior area. Third, several previous studies assessed the alpha angle using computed tomography combined with MRI [2, 3]. However, our study did not include computed tomography assessment to avoid exposing the patients to radiation [4]. Fourth, as all patients

included in this study had hip pain, there was an inherent bias to identify FAI-related findings. Especially, positive and negative predictive values are dependent on prevalence. When generalising the findings to the community setting, care should be taken as the high prevalence of the disease could distort the results of positive and negative predictive values.

With regard to the clinical relevance of this diagnostic study, evaluation of cam deformity using the 45° Dunn view would be useful in screening for cam deformity when using radiography, which is the standard to evaluate bony abnormalities. In epidemiological research, evaluation using only the AP pelvis view may be inadequate to screen for cam deformity [13]. Thus, the results presented here have important implications for such studies.

Conclusions

The 45° Dunn view was most closely correlated to radial MRI slices compared with the AP pelvis, cross-table lateral, 90° Dunn and modified 45° Dunn views. The 45° Dunn view had greater sensitivity than other radiographic projections.

References

1. Barton C, Salineros MJ, Rakhra KS, Beaulé PE (2011) Validity of the alpha angle measurement on plain radiographs in the evaluation of cam-type femoroacetabular impingement. Clin Orthop Relat Res 469:464–469
2. Beaulé PE, LeDuff M, Zaragoza EJ (2007) Quality of life following femoral head-neck osteochondroplasty for femoroacetabular impingement. J Bone Joint Surg Am 89:773–779
3. Beaulé PE, Zaragoza E, Motamedi K, Copelan N, Dorey FJ (2005) Three-dimensional computed tomography of the hip in the assessment of femoroacetabular impingement. J Orthop Res 23:1286–1292
4. Berrington de González A, Darby S (2004) Risk of cancer from diagnostic X-rays: estimates for the UK and 14 other countries. Lancet 363:345–351
5. Clohisy JC, Carlisle JC, Beaulé PE, Kim YJ, Trousdale RT, Sierra RJ, Leunig M, Schoenecker PL, Millis MB (2008) A systematic approach to the plain radiographic evaluation of the young adult hip. J Bone Joint Surg Am 90(Suppl 4):47–66
6. Clohisy JC, Carlisle JC, Trousdale RT, Kim Y-J, Beaule PE, Morgan P, Steger-May K, Schoenecker PE, Millis M (2009) Radiographic evaluation of the hip has limited reliability. Clin Orthop Relat Res 467:666–675

7. Domayer SE, Ziebarth K, Chan J, Bixby S, Mamisch TC, Kim YJ (2011) Femoroacetabular cam-type impingement: diagnostic sensitivity and specificity of radiographic views compared to radial MRI. Eur J Radiol 80:805–810

8. Dudda M, Albers C, Mamisch TC, Werlen S, Beck M (2009) Do normal radiographs exclude asphericity of the femoral head-neck junction? Clin Orthop Relat Res 467:651–659

9. Dunn DM (1952) Anteversion of the neck of the femur; a method of measurement. J Bone Joint Surg Br 34:181–186

10. Ganz R, Leunig M, Leunig-Ganz K, Harris WH (2008) The etiology of osteoarthritis of the hip: an integrated mechanical concept. Clin Orthop Relat Res 466:264–272

11. Ganz R, Parvizi J, Beck M, Leunig M, Nötzli H, Siebenrock KA (2003) Femoroacetabular impingement: a cause for osteoarthritis of the hip. Clin Orthop Relat Res 417:112–120

12. Klenke FM, Hoffmann DB, Cross BJ, Siebenrock KA (2015) Validation of a standardized mapping system of the hip joint for radial MRA sequencing. Skeletal Radiol 44:339–343

13. Laborie LB, Lehmann TG, Engesæter IØ, Eastwood DM, Engesæter LB, Rosendahl K (2011) Prevalence of radiographic findings thought to be associated with femoroacetabular impingement in a population-based cohort of 2081 healthy young adults. Radiology 260:494–502

14. Larson CM (2010) Arthroscopic management of pincer-type impingement. Sports Med Arthrosc 18:100–107

15. Leunig M, Podeszwa D, Beck M, Werlen S, Ganz R (2004) Magnetic resonance arthrography of labral disorders in hips with dysplasia and impingement. Clin Orthop Relat Res 418:74–80

16. Leunig M, Werlen S, Ungersbock A, Ito K, Ganz R (1997) Evaluation of the acetabular labrum by MR arthrography. J Bone Joint Surg Br 79:230–234

17. Meyer DC, Beck M, Ellis T, Ganz R, Leunig M (2006) Comparision of six radiographic projections to assess femoral head/asphericity. Clin Orthop Relat Res 445:181–185

18. Nötzli HP, Wyss TF, Stoecklin CH, Schmid MR, Treiber K, Hodler J (2002) The contour of the femoral head-neck junction as a predictor for the risk of anterior impingement. J Bone Joint Surg Br 84:556–560

19. Pfirrmann CW, Mengiardi B, Dora C, Kalberer F, Zanetti M, Hodler J (2006) Cam and pincer femoroacetabular impingement characteristic MR arthrographic findings in 50 patients. Radiology 240:778–785

20. Tanzer M, Noiseux N (2004) Osseous abnormalities and early osteoarthritis: the role of hip impingement. Clin Orthop Relat Res 429:170–177